Molecular level structural studies of metalloproteins/metalloenzymes by scanning tunnelling microscopy: Scopes and promises

R. Mukhopadhyay

Department of Biological Sciences and Bioengineering, Indian Institute of Technology, Kanpur 208 016, India

Structural studies of various metalloproteins and metalloenzymes have been carried out at molecular level by scanning tunnelling microscopy (STM) in the last few years. The potential, limitations and essential requirements for effective STM investigations of protein structures are discussed in this article with specific examples of four electron transfer proteins/enzymes azurin, rubredoxin, putidaredoxin and cytochrome $P450_{cam}$ and a number of other proteins/enzymes studied by STM over the past 15 years.

SINCE the invention of scanning tunnelling microscopy (STM) in 1982 by Binnig and Rohrer[1,2], there is a sustained effort to extend the application of this technique from the domain of studying conductors and semiconductors to insulators/quasi-conductors like proteins and enzymes. The discovery in 1986, that STM could be operated under fluid[3,4] opened the possibility of high-resolution studies of biomolecules in a near-physiological condition. A wide range of biological systems, starting from small biomolecules like DNA bases and their derivatives[5–9], amino acids and peptides[10–13] to proteins[14–26] have been imaged since then. Several reports on protein films, e.g. catalase[17,19], lysozyme[18], cytochrome C[23], azurin[20–22,24,25] and cytochrome[26] P450 as well as individual isolated molecules with molecular[14–16,27–33] and sub-molecular[14–16] resolution have been made. There has been significant progress in STM studies of proteins, both in static conditions and in 'real time'[34], with advancements in immobilization techniques[16,34] and ability for interpretation of the image contrast[35–37].

Among the family of scanning probe microscopy (SPM) techniques, atomic force microscopy (AFM) is popularly used for imaging biomolecules[38,39] and has emerged as a versatile technique to study insulators and quasi-conductors in general. In AFM, the variation in force operating between the probe and the sample is monitored and translated into surface features[40]. However, the typical spatial resolution that can be obtained from AFM is less than that of STM. Lateral resolution of 1 Å and vertical resolution of 0.1 Å are obtainable from STM studies, whereas the resolution in AFM is generally not more than 5 Å and 0.5 Å along x–y and z-axes respectively. Distortion of molecular shape/size of isolated protein molecules as a result of tip–sample interactions associated with large tip–sample contact area is unavoidable during AFM imaging. Larger dimensions than predicted from X-ray/NMR data are a usual observation in AFM because of convolution between the probe size/shape and sample features. These effects of an AFM probe on the molecular shape/dimension can be less prominent, when the molecule is surrounded by other molecules as it is in the close packed situation and is three dimensionally trapped at the interface. On the contrary, in case of STM imaging, sample distortion is much less since the probe is sharper than AFM probe and isolated molecules and protein adlayers can be imaged more reliably. Of course, there are situations where the use of AFM may provide valuable information. For example, force spectroscopic measurements on single molecules can be made to understand the process of protein folding in mechanically stable proteins[41–44]. Also, resolution of AFM can be enhanced and sample damage can be minimized by imaging with an oscillating cantilever where oscillation is induced in the alternating current mode (AC mode) either by an acoustic signal (AAC mode)[45] or a magnetic signal (MAC mode)[46].

The extraordinary benefits STM/AFM can offer for studying proteins/enzymes are the following: (i) STM/AFM can be used universally, since proteins of variable sizes can be studied; (ii) direct 3-dimensional information can be obtained at angstrom order resolution in a short period of time, usually a few minutes, and (iii) a flexible experimental medium (vacuum, ambient/gaseous and fluid) ensures structural characterization of proteins in the near native environment.

These benefits were hitherto unavailable with a single individual technique, since the protein must be crystallized for X-ray diffraction studies, protein size has to be limited for reliable data interpretation in NMR studies, physiological conditions cannot be maintained in a cryo-EM experiment and sample dehydration/metallic coating is essential in case of transmission electron microscopy (TEM) studies.

e-mail: rupam@iitk.ac.in

STM has been preferred over AFM by several research groups for certain advantages, e.g. unparalleled resolution and minimum distortion of molecular size and shape. Reports on molecular level imaging of single phosphorylase kinase and phosphorylase *b*[29] and immunoglobulin G[30] made as early as in 1991 showed STM's potential to provide shape information on single protein molecules. A number of structural studies on single protein molecules have been made afterwards and it has been noticed in recent time that the search for location of high contrast site(s), e.g. metal centre(s) within a metalloprotein or a metalloenzyme molecule is greatly aided by the application of STM[14–16]. Apart from structural benefits, a combination of spectroscopic [scanning tunnelling spectroscopy (STS)][47–54] and/or electrochemical experiment[55] along with high resolution imaging can lead to a wealth of data on electron transfer properties of single metalloprotein/metalloenzyme molecules and protein films[56–58]. Overall, the promises of application of STM in studying structural and conformational details of functional protein molecules at different interfaces are evident and it is to be seen that with advancements in instrumentation, immobilization methods and capabilities to explain image contrast, STM affirms its place as a valuable technique for protein structure analysis.

Operational principles of STM

In STM, a conductive probe is brought very close (5–50 Å) to a conductive sample, a voltage difference (bias voltage) is applied between the two, and the tunnel current as a result of electron tunnelling between the probe and sample is monitored in real space and time (Figure 1). Tunnel current (I) is expressed as

$$I = AV \exp(-2\kappa d),$$

where V is the bias voltage, d the probe–sample separation, A the parameter depending on local density of state at Fermi level of the sample and the tip, and κ is the decay constant of a sample state near Fermi level in the barrier region.

The changes in tunnel current as sensed by an electronic feedback system can be translated into an image of surface features either in 'constant height' or in 'constant current' mode. In the constant height mode, probe sample separation is kept fixed and changes in tunnel current are measured. In the latter, tunnel current is kept constant at a reference value by an electronic feedback system and changes in probe–sample separation along z-axis are monitored. A region of brighter contrast means higher tunnel current in the constant height mode and higher topographic features in the constant current mode. A negative contrast may indicate lower tunnel current/indentations and asymmetric tip related artifacts. It is expected that the electronic structure be probed in constant height mode, while the topographic features are imaged in constant current mode. In practice, a convolution between the electronic and topographic features with a predominance of either dictates final mage formation[59]. Some important parameters that control relative influence of electronic structure and topographic features are thought to be tunnel current, bias voltage, environmental conditions, probe shape/size, adsorbate–substrate interactions, probe–adsorbate interactions and the presence of electronically accessible moieties in the molecule. Constant current mode is usually preferred in morphological studies for reasons related to stable imaging and relative ease of interpretation of the image contrast.

Important factors for effective imaging of protein molecules

Though protein imaging at high resolution by STM is still at an early stage, notable progress has been made to understand the basic requirements for imaging single protein molecules. Necessity of structural stability of the protein molecule, adsorption with specific orientation, indirect adsorption and specific location of the metal site for successful STM imaging of protein molecules at high resolution are exemplified and discussed in the following sections with specific examples of the electron transfer

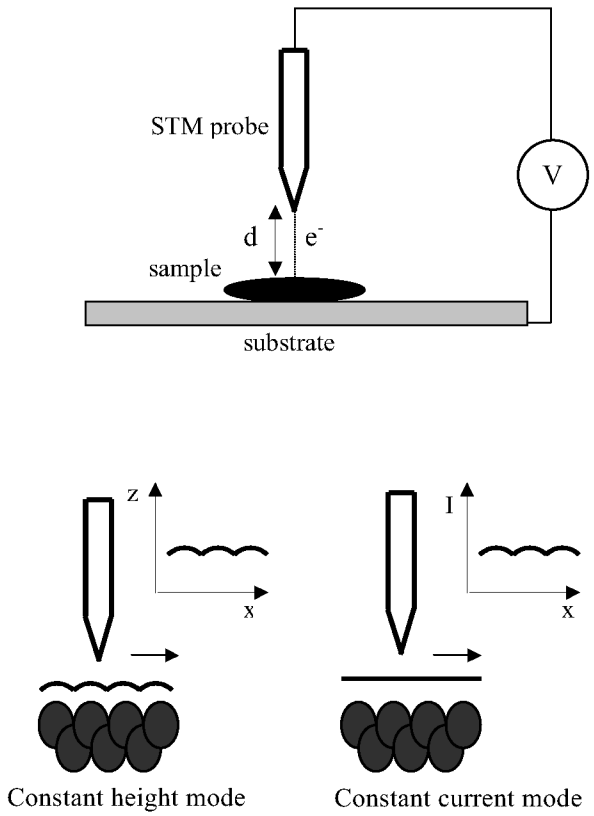

Figure 1. A schematic of STM operation.

proteins azurin (a copper protein from *Pseudomonus aeruginosa*), rubredoxin (an iron-sulphur protein from *Clostridium pasteurianum*), putidaredoxin (an iron-sulphur protein from *Pseudomonus putida*) and cytochrome $P450_{cam}$ (a mono-oxygenase heme enzyme from *Pseudomonus putida*).

Structural stability

Adsorption-induced damages and probe-induced damages are generally unavoidable in an SPM study of soft biological samples. Effective studies can be made only on structurally robust proteins that are able to withstand mechanical stresses due to adsorption and action of scanning probe, and electrical stresses due to high voltages applied for imaging soft biological molecules.

Azurins are well-characterized type I blue copper proteins[60]. They act as electron transport agent/electron bridge in biological electron transfer chains, e.g. bacterial denitrification. Their role as electron transport mediators has prompted investigations on interactions between an electrode and the protein molecules in an artificial environment. Adsorption studies on azurin exhibit high degree of structural stability, which is also reflected in its functional integrity in adsorbed state[37]. In Figure 2 *a*, an STM image of isolated azurin molecules adsorbed on gold electrode surface is presented. These molecules appear quasi-spherical and quite accurate dimensional match with the X-ray structure (length ~ 35 Å and width ~ 25 Å) (Figure 2 *b*) is also evident. Stable and clear imaging, and similarity of the image shape and dimension to the X-ray structure indicate minimum structural distortion during adsorption and scanning. This protein is used these days as a model system for studying electron transfer processes between an electrode and a metalloprotein at molecular level[37].

Oriented adsorption

It has been found that 'reproducible' imaging of single protein molecules at high resolution heavily depends on the orientation of the molecules. Different molecules can adopt different orientations at an interface, resulting in observation of a variety of shapes and dimensions. This is inevitable especially when a suitable anchoring arrangement to immobilize the molecules in an oriented manner is not present. The effects of oriented immobilization or a lack of it are exemplified in the following paragraphs.

C. pasteurianum rubredoxin is a small protein of length ~ 28 Å and width ~ 25 Å. It has a single iron coordinated to the sulphur atoms of four cysteine residues near one edge of the molecule[61]. A characteristic image of isolated rubredoxin molecules shows mostly spherical and elliptical shapes as also predicted from X-ray studies (Figure 3 *a*, *b*). However, a variation in both size and shape is evident in this figure that indicates random orientation of the adsorbed molecules. Effects of random molecular orientation on the image shape were observed for other systems, e.g. cytochrome $P450_{cam}$ (CYP101) too. Two molecules shown in Figure 4 *a* and *b* reveal close similarity with the X-ray structure of the substrate-free enzyme[62]. Both triangular front face (50 Å × 50 Å × 60 Å) (Figure 4 *a*) and elliptical side face (50/60 Å × 30 Å) (Figure 4 *b*) are observed with clear indication of even the clefts. However, in spite of STM's capability of providing shape information, the observation of two widely different shapes indicates irreproducibility in imaging of a particular shape as a consequence of random orientation associated with non-specific adsorption.

A different effect of random molecular orientation is evident from Figure 3. An internal feature is observed in two molecules out of 15. It is plausible that these sub-molecular features appear when the molecules are adsor-

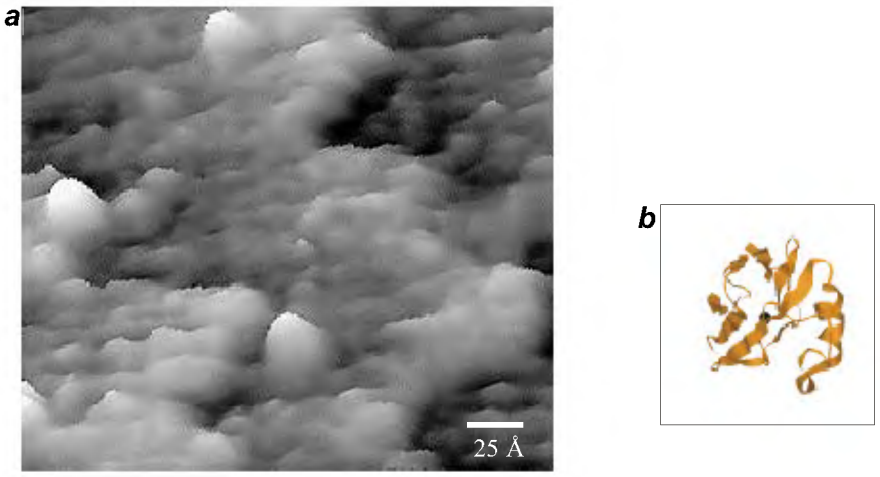

Figure 2. ***a***, Single azurin molecules on gold electrode surface (I_t = 0.4 nA; V_b = – 800 mV; *Z*-range = 0–6.5 Å). ***b***, X-ray structure of *Pseudomonus aeruginosa* azurin.

bed with a specific orientation. This could have been a matter of chance, as many orientations can exist in the absence of a suitable anchoring arrangement. Similar effect of non site-specific adsorption was observed for metallothionein[14] as well, where the internal features located on seven zinc–sulphur moieties were observed in one molecule out of several.

A number of immobilization techniques mostly based on electrostatic compatibility between the substrate surface and protein molecules have been developed over the past few years[63–66]. Various methods involving substrate modification by covalently attached linker molecules, substrate anodization/cathodization by electrochemical means, modification of charged substrate by ionic species and use of charged lipid films were exploited. These methods were mostly successful as far as non-specific adsorption is concerned. A method for 'site-specific' immobilization of the protein molecules has been proposed recently[16,34]. In this method, a cysteine residue is introduced at a suitable position of the protein surface by conservative mutagenesis followed by chemisorption of the mutant molecules on gold electrode surface via strong gold–thiol interaction[67]. A stark contrast in adsorption behaviour between wild type putidaredoxin (pdx) and C73S-D58C, a thiolated mutant of pdx was observed (Figures 5 and 6). Significant variation in molecular shape/size as a result of random orientation of pdx (wild type) molecules is observed in Figure 5, while a great similarity in shape and dimension for most of the molecules was a routine observation for the mutant molecules (Figure 6 *a*, *b*). A close similarity in shape and dimension with NMR structure is evident from the STM image shown in Figure 6 *b*. Amongst the many existing techniques for protein immobilization, this appears to be site-specific with consequence in predetermination of orientation[16] and functional control as far as electron transfer processes between immobilized protein molecules and electrode surface is concerned.

Immobilization with minimum surface contact

Direct adsorption of protein molecules on a metal surface almost always results in drastic and undesirable conformational changes leading to modifications/complete loss of function. Structural damages associated with such conformational changes are usually expressed in enlargement

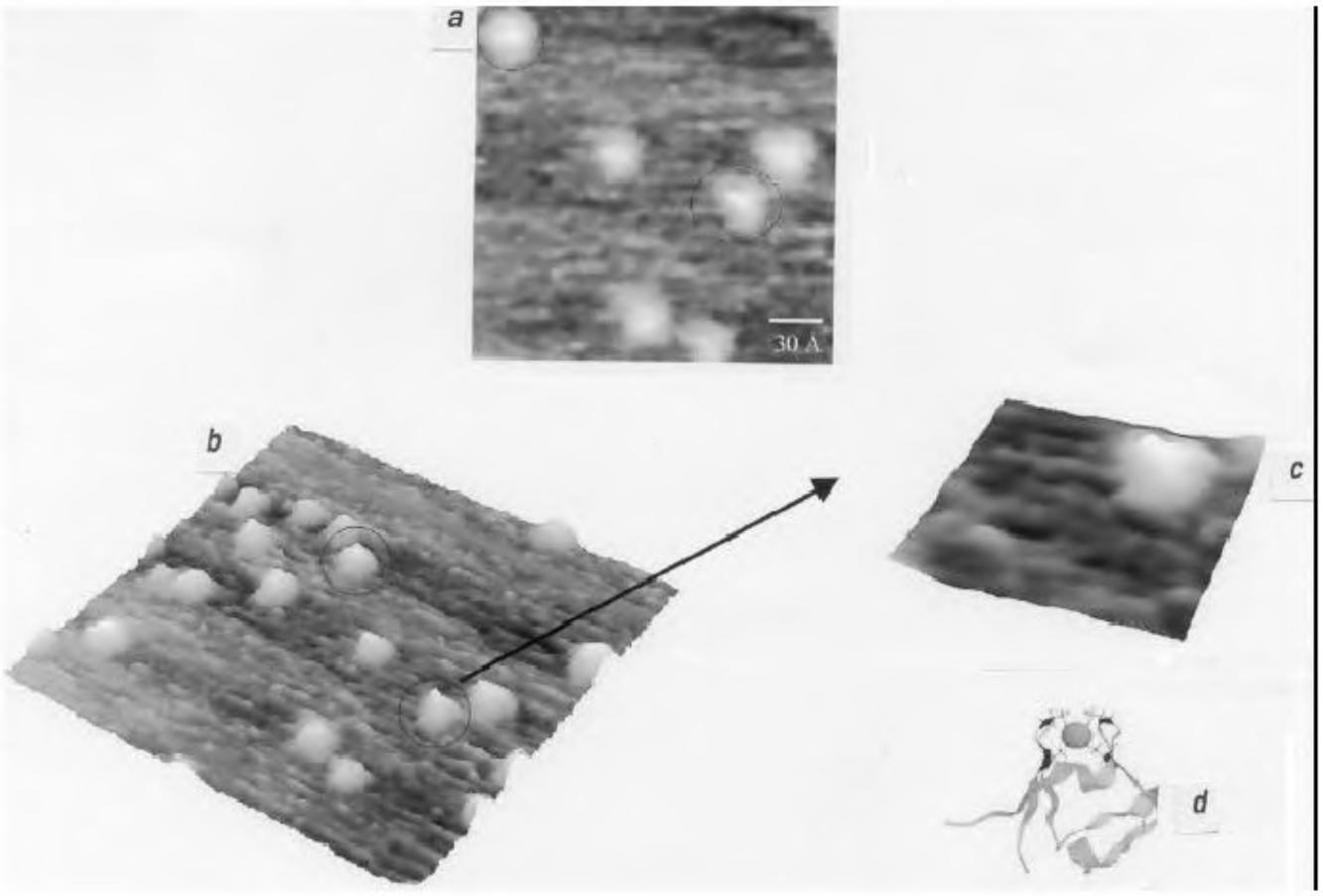

Figure 3. (***a***) Top view and (***b***) 3-d view of isolated molecules of rubredoxin at gold–water interface – sub-molecular contrast is observed in two highlighted molecules (I_t = 0.2 nA; V_b = 900 mV; *z*-range = 0–6 Å). ***c***, Magnified image of one of the highlighted molecules in (***b***) (I_t = 200 pA; V_b = 900 mV; scan range = 110 × 110 Å; *z*-range = 0–6 Å). ***d***, X-ray structure of *Clostridium pasteurianum* rubredoxin.

of size and distortion of the molecular shape. Adsorption-induced damages are evident in the STM images of rubredoxin and putidaredoxin molecules presented in Figures 3 and 5 respectively. The molecule shown in Figure 3 *c* appears larger (~ 35 Å in length) than the size predicted from X-ray studies. Majority of the pdx molecules (Figure 5) also appear bigger compared to the NMR dimensions, i.e. 35 Å × 18 Å. Similar size enlargement was observed earlier for immunoglobulin G, phosphorylase kinase and phosphorylase *b* too by STM studies[29,30].

It is understood that the adsorption-induced damages can be minimized by minimizing physical contact of the protein molecules with substrate surface. At the same time, immobilization is essential for stable and successful imaging. C73S-D58C, the pdx mutant discussed earlier was used for generating 'single point contact' with the gold electrode surface by the formation of a gold–thiol bond. Dimensional similarity with NMR structure as observed in the images of mutant molecules (Figure 6 *b*) indicates 'indirect' adsorption through minimum surface contact(s), resulting in preservation of solution state structure in adsorbed state. A direct application of such non-destructive immobilization method was realized in the formation of a surface confined complex (Figure 7 *a*) between immobilized single pdx mutant (C73S-D58C) molecule and a single CYP101 molecule at gold–water interface[16]. Striking structural similarity with the presumed electron transfer complex is evident from a comparison between the STM image and the molecular dynamics simulation model[68] (Figure 7 *b*). Stability of the adsorbed complex is achieved by means of electrostatic association of CYP101 with pdx molecules via salt bridges, hydrogen bonds and hydrophobic contacts, while the enzyme molecule remains physisorbed via contacts through one of its elliptical faces. A close similarity between the simulated model and STM image of the complex indicates minimal damage of the molecules when they form a complex and remain adsorbed on the gold surface.

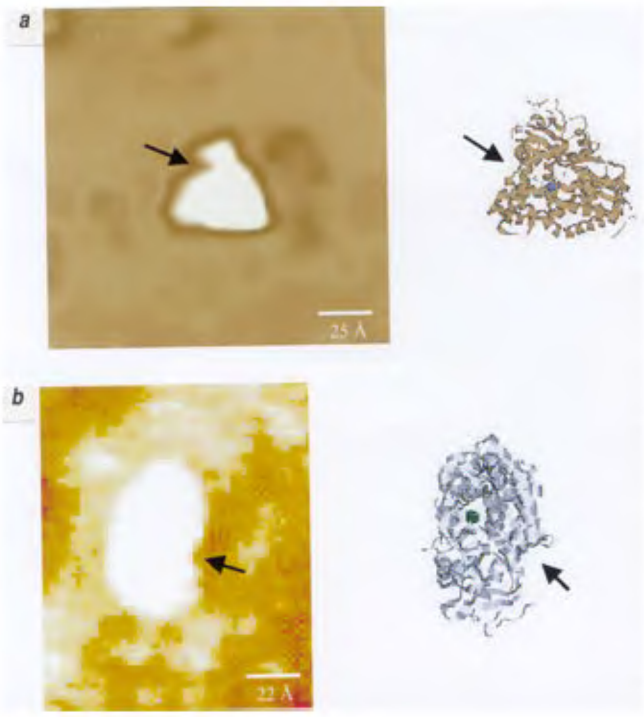

Figure 4. A comparison between STM images of single molecules of cytochrome P450 and its crystal structure (the clefts are indicated by arrows) (I_t = 0.26 nA; V_b = 1260 mV; *z*-range = 0–19 Å). ***a***, triangular front face and, ***b***, elliptical side face.

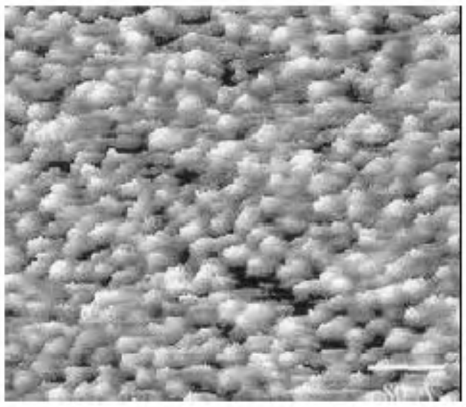

Figure 5. A high coverage of putidaredoxin molecules at gold–water interface (I_t = 0.5 nA; V_b = – 500 mV; *z*-range = 0–10 Å).

Elimination of artifacts

Artifacts related to contamination, noise, improper scan parameters and wrong use of image processing software can lead to features that appear as real[59] and prevent effective structural studies of proteins by STM. Stringent control experiments should be performed by studying freshly prepared substrate surface either in ambient conditions and/or imaging under the same fluid using similar scan parameters as used in experiments with the protein solutions. The effects of random and periodic noise should be minimized by controlling various sources of noise, e.g. building vibration, acoustic vibration, thermal fluctuations, electronic, etc. Application of optimized scan parameters and proper use of image processing software can also reduce anomalies to a large extent.

Spatial resolution

Resolution in STM ideally implies detection/measurement of tunnel current at each pixel on X–Y plane by an atomically sharp probe. In practice, it is a collective result over a few atoms of the probe end leading to lower resolution. A mismatch between the probe size and pixel-to-pixel separation can also result in reduced resolution. Lateral resolution in STM is primarily determined by probe dimension and probe shape[69], while the exquisite resolution in *z*-axis is controlled by the exponential dependence of tunnel current on probe–sample separation. Other fac-

tors influencing the lateral resolution are translational/rotational mobility of the adsorbed molecules, molecular structural motion, humidity/hydration and tunnel resistance/tip–sample separation[59].

Contrast formation

The major hurdle in STM studies of protein molecules is the interpretation of tunnel profiles. Protein molecules are well-known insulators/quasi-conductors with high resistivity, typically 10^{15}–10^{18} Ω m at room temperature[70]. They appear to behave as passive molecules like a spacer between two electrodes[71] and one can argue that the concept of vacuum tunnelling[72] be applied in this case, when the spacer is expected to be non-interfering during tunnelling. However, the achievements in protein imaging indicate that STM can sense these quasi-conductors. Visualization of the molecular shape during STM imaging indicates flow of electrons from outer surface of the molecule, while observation of an internal feature may mean electron flow from the outer boundary, e.g. in case of rubredoxin[15], where the iron–sulphur site is solvent-exposed and/or through the molecule, e.g. in case of metallothionein[14] and cytochrome[16] P450. The latter two examples reflect an active role of the molecule[73–80] in tunnelling mechanism though under normal STM operation, the electrons are supposed to tunnel between the probe and the sample without interfering with the molecular states[81].

Image contrast of protein molecules can be difficult to understand when the images are obtained in fluid phase. Tunnelling through a molecular–liquid medium[82–84] is complicated as there can be static and fluctuational effects due to water molecules trapped in the tunnel gap and a non-exponential tunnelling near the electrode has been proposed[85]. The electric current measured during protein imaging may include contributions from electronic, ionic[86] and protonic surface conduction[86,87] and involve electron flow across covalent or hydrogen bonds and van der Waals contacts within the protein structure[88]. For example, in rubredoxin, aromatic groups like phenyl alanine, tyrosine and tryptophan are distributed within the central cavity of the molecule. Although they display several orientations, the side chain rings are virtually in contact with each other and with the FeS_4 active site, providing a possible extended pathway for electronic interaction of the iron site with the underlying gold electrode surface. Resonance between the unoccupied levels of unperturbed molecules and the probe Fermi level is unlikely as proteins have a large band gap (5–7 eV)[89]. It is, however, possible that pressure within the tunnel gap[90], moves the molecular energy levels and subsequently makes them accessible to the metallic Fermi levels. Tip-induced compression of the adsorbate can lead to a strong amplification of tunnel current by perturbation of

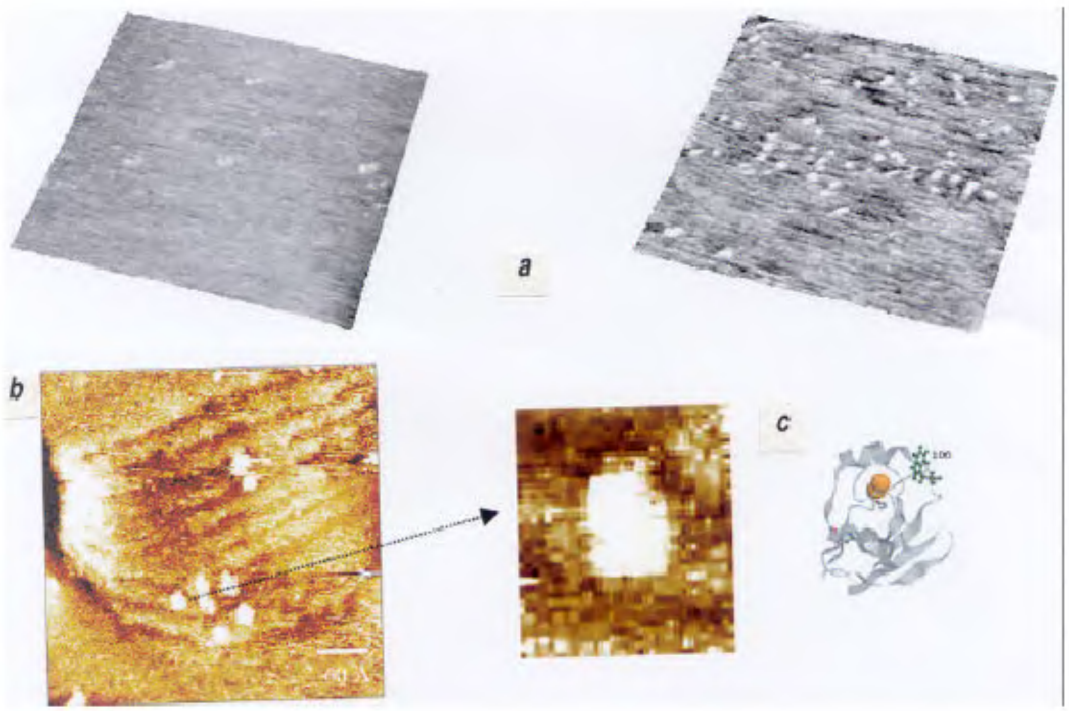

Figure 6. ***a***, Adsorption of C73S-D58C monitored at a time interval of 30 min at gold–buffer interface (I_t = 0.7 nA; V_b = – 700 mV; scan range = 860 × 860 Å; z-range = 0–20 Å). ***b***, Individual molecules of pdx mutant immobilized on gold surface (I_t = 1.023 nA; V_b = 800 mV; z-range = 0–9.9 Å). ***c***, A comparison between the imaged shape of a molecule immobilized with Trp 106 solution exposed and the expected shape from NMR structure.

the electronic structure of the molecule. Also, nuclear configurational fluctuations[37], and any perturbation of the metal centre by means of ligation and by the electric field of immediate protein environment may help in bringing the energy level(s) near the substrate/probe Fermi level and therefore, resulting in a near-resonance situation. The role of metal atomic orbital in contrast enhancement, e.g. in case of rubredoxin[15], especially when one considers direct interaction between the scanning tip and the metal center that is not deeply embedded in protein matrix but located near the protein surface[91] (Figure 3) can be important. It is possible that the sulphur atoms also contribute to tunnel enhancement by means of their relatively high atomic polarizability[92]. Enhanced tunnelling associated with sulphur atoms has been reported in organic films earlier[93] and it has been argued that functional group contrast can be related to their ionization potential indicative of hole transfer[37]. Interactions of ligand sulphur atoms with underlying gold surface has also been proposed to be responsible for contrast enhancement over zinc–sulphur sites in metallothionein molecule[14]. A role of 'through space' tunnelling between an electron-rich unit buried inside the protein matrix and scanning probe and/or a role of relevant amino acid residues situated on the electron transfer pathway may also be considered to justify the contrast observed in some cases, e.g. cytochrome $P450_{cam}$ (ref. 16).

Future directions

A great similarity is observed between the NMR/X-ray structure of a protein and its STM image wherever the conditions are optimized for least damage of the adsorbed molecules. These findings may encourage one to carry out STM investigations on proteins/enzymes of unknown structure. As mentioned before, NMR or X-ray structure cannot be obtained for many proteins because of sample preparation difficulties or difficulties in interpretation of the data. Information regarding dimension, shape, structural stability and monomeric/multimeric state can be obtained from STM studies. Studies on proteins of unknown structure are underway by the author at present.

Though STM shows promise in revealing tertiary structure of a protein, the present level of instrumental capabilities do not allow an STM experimentalist to achieve the level of internal resolution obtainable from X-ray/NMR studies. Development of more sensitive pre-ampli-

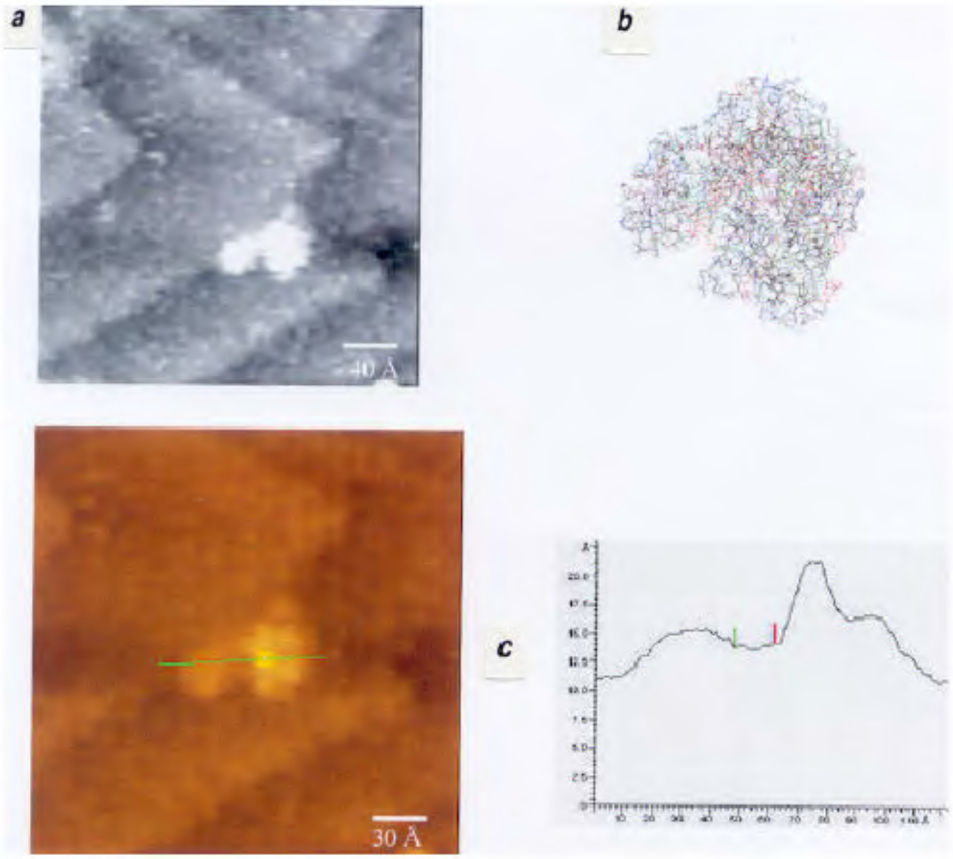

Figure 7. ***a***, STM image of the proposed electron transfer complex between putidaredoxin and cytochrome P450 at gold(111)–water interface (I_t = 0.2 nA; V_b = – 0.7 V; z-range = 0–8 Å). ***b***, Molecular dynamics simulation model of the complex. ***c***, Sub-molecular contrast in cytochrome P450 molecule: intermolecular separation is ~ 14 Å as shown in the cross-sectional analysis.

fiers to detect currents of femptoamp or even lower range should help resolve positions of electronically addressable atoms/groups like nitrogen, phosphorus, sulphur, alkene, alkyne, aromatic groups and metal centres with convenience. Working at a low temperature should also help in increasing lateral resolution, since mobility of the molecules can be reduced and immobilization be aided leading to sub-molecular resolution.

A limitation in structural studies of protein molecules by STM is that the STM image of a protein molecule can be obtained only when the molecule is adsorbed in an interface. Though good resemblance between X-ray/NMR structure and STM image is observed often, it is still questionable how often one can reliably compare the X-ray/NMR structure with an STM image of an adsorbed protein molecule, given the adsorption-induced distortions mentioned before. To minimize this problem, one may use an immobilization technique where contact area between the surface and the molecule is minimum.

Some interesting future works would be to replace the iron atom(s) in iron–sulphur proteins by other sulphur-binding metal(s) (e.g. zinc or cadmium) and then image at high resolution to see whether metal replacement leads to any change in contrast over high contrast area(s). Such work should have important implications in differentiating different metal centres within a single multicentred molecule that may help in understanding electron transfer properties of multicentred metalloproteins/metalloenzymes at 'single molecule' level. Also, the ability of STM to image a surface-confined complex between a protein molecule and an enzyme molecule[16] that is its redox partner, can be the beginning of the dream of 'molecular enzyme sensor' being realized. Experiments with electrochemical potential control and use of scanning tunnelling spectroscopy to observe the effects of 'intracomplex' 'intermolecular' 'direct' electron transfer need to be carried out to fulfill this dream.

Though immobilization of a protein molecule via gold–thiol bond formation appears to be successful for a small protein like pdx, it is yet to be seen whether the same method would lead to successful immobilization of bigger enzyme molecules. More than one thiol may be necessary for keeping the enzyme molecules immobilized on substrate surface over an appreciably long residence time. Effective immobilization via gold–thiol bond formation should be reflected in the similarity of observed shape for all the molecules in an adlayer generated by the same mutant. Of course, the ultimate success of effective immobilization would depend on the relatively defect-free nature of substrate surface that would ensure similar local adsorption environment for a majority of the molecules. Care should also be taken not to immobilize the enzyme molecule through thiol(s) incorporated near active site since that may change enzyme function drastically. Finally, investigations with other techniques like X-ray photoelectron spectroscopy (XPS)/surface enhanced resonance Raman spectroscopy (SERS) should be made before the use of the thiolated mutants can be established in technological applications.

1. Binnig, G. and Rohrer, H., *Helv. Phys. Acta*, 1982, **55**, 726–735.
2. Binnig, G., Rohrer, H., Gerber, Ch. and Weibel, E., *Phys. Rev. Lett.*, 1982, **49**, 57–61.
3. Sonnenfeld, R. and Hansma, P. K., *Science*, 1986, **232**, 211–213.
4. Liu, H. Y., Fan, F.-R. F., Lin, C. W. and Bard, A. J., *J. Am. Chem. Soc.*, 1986, **108**, 3838–3839.
5. Lindsay, S. M., Thundat, T., Nagahara, L., Knipping, U. and Rill, R. L., *Science*, 1989, **244**, 1063–1064.
6. Lindsay, S. M., Tao, N. J., DeRose, J. A., Oden, P. I., Lyubchenko, Yu. L., Harrington, R. E. and Shlyakhtenko, L., *Biophys. J.*, 1992, **61**, 1570–1584.
7. Wandlowski, Th., Lampner, D. and Lindsay, S. M., *J. Electroanal. Chem.*, 1996, **404**, 215–226.
8. Srinivasan, R., Murphy, J. C., Fainchtein, R. and Pattabiraman, N., *J. Electroanal. Chem.*, 1991, **312**, 293–297.
9. Tao, N. J. and Shi, Z., *J. Phys. Chem.*, 1994, **98**, 1464–1471.
10. Katsumata, S. and Ide, A., *Jpn. J. Appl. Phys.*, 1995, **34**, 3360–3365.
11. Davies, M. C., Jackson, D. E., Price, M. R. and Tendler, S. J. B., *Cancer Lett.*, 1990, **55**, 13–16.
12. Coratger, R., Chahboun, A., Ajustron, F., Beauvillain, J., Erard, M. and Amalric, F., *Ultramicroscopy*, 1990, **34**, 141–147.
13. Dakkouri, A. S., Kolb, D. M., Edelstein-Shima, R. and Mandler, D., *Langmuir*, 1996, **12**, 2849–2852.
14. Davis, J. J., Hill, H. A. O., Kurz, A. C., Jacob, W. Maret and Vallee, B. L., *Phys. Chem. Commun.*, 1998, Article 2.
15. Mukhopadhyay, R., Meyer, J., Kyritsis, P., Davis, J. J. and Hill, H. A. O., *J. Inorg. Biochem.*, 2000, **78**, 251–254.
16. Mukhopadhyay, R., Lo, K. K., Wong, L. L., Pochapsky, T. and Hill, H. A. O., *Phys. Chem. Chem. Phys.*, 2002, **4**, 641–646.
17. Leggett, G. J., Davies, M. C., Jackson, D. E., Roberts, C. J., Tendler, S. J. B. and Williams, P. M., *J. Phys. Chem.*, 1993, **97**, 8852–8854.
18. Haggerty, L. and Lenhoff, A. M., *Biophys. J.*, 1993, **64**, 886–895.
19. Parker, M., Davies, M. C. and Tendler, S. J. B., *J. Phys. Chem.*, 1995, **99**, 16155–16161.
20. Andersen, J. E. T., Møller, P., Pedersen, M. V. and Ulstrup, J., *J. Surf. Sci.*, 1995, **325**, 193–205.
21. Andersen, J. E. T., Olesen, K. G., Danilov, A. I., Foverskov, C. E., Møller, P. and Ulstrup, J., *J. Bioelectrochem. Bioenerg.*, 1997, **44**, 57–63.
22. Friis, E. P., Andersen, J. E. T., Madsen, L. L., Møller, P. and Ulstrup, J., *J. Electroanal. Chem.*, 1997, **431**, 35–38.
23. Zhang, B. and Wang, E., *J. Chem. Soc., Faraday Trans.*, 1997, **93**, 327–331.
24. Friis, E. P., Andersen, J. E. T., Kharkats, Y. I., Kuznetsov, A. M., Nichols, R. J., Zhang, J. D. and Ulstrup, J., *Proc. Natl. Acad. Sci. USA*, 1999, **96**, 1379–1384.
25. Chi, Q., Zhang, J., Nielsen, J. U., Friis, E. P., Chorekendorff, I., Canters, G. W., Andersen, J. E. T. and Ulstrup, J., *J. Am. Chem. Soc.*, 2000, **122**, 4047–4055.
26. Davis, J. J., Hill, H. A. O. and Bond, A. M., *Coord. Chem. Rev.*, 2000, **411**, 200–210.
27. Feng, L., Hu, C. Z. and Andrade, J. D., *J. Colloid Interface Sci.*, 1988, **126**, 650–653.
28. Edstrom, R. D., Meinke, M. H., Yang, X., Yang, R. and Evans, D. F., *Biochemistry*, 1989, **28**, 4939–4942.
29. Lee, G., Evans, D. F., Elings, V. and Edstrom, R. D., *J. Vac. Sci. Technol. B*, 1991, **9**, 1236–1241.
30. Leatherbarrow, R. J., Stedman, M. and Wells, T. N. C., *J. Mol. Biol.*, 1991, **221**, 361–365.

31. Chi, Q., Zhang, J., Dong, S. and Wang, E., *J. Chem. Soc., Faraday Trans.*, 1994, **90**, 2057–2060.
32. Zhang, J. D., Chi, Q., Dong, S. J. and Wang, E., *J. Electroanal. Chem.*, 1994, **379**, 535–539.
33. Zhang, J., Chi, Q., Dong, S. and Wang, E., *Bioelectrochem. Bioenerg.*, 1996, **39**, 267–274.
34. Davis, J. J., Halliwell, C. M., Hill, H. A. O., Canters, G. W., van Amsterdam, M. C. and Verbeet, M. Ph., *New J. Chem.*, 1998, **1**, 1119–1123.
35. Lindsay, S. M., Jing, T. W., Pan, J., Vaught, A. and Rekesh, D., *Nanobiology*, 1994, **3**, 17–27.
36. Friis, E. P., Kharktas, Y. I., Kuznetsov, A. M. and Ulstrup, J., *J. Phys. Chem. A*, 1998, **102**, 7851–7859.
37. Zhang, J. *et al.*, *J. Phys. Chem. B*, 2002, **106**, 1131–1152.
38. Bustamante, C. and Rivetti, C., *Annu. Rev. Biophys. Biomol. Struct.*, 1996, **25**, 395–429.
39. Hansma, H. G., *Annu. Rev. Phys. Chem.*, 2001, **52**, 71–92.
40. Binnig, G., Quate, C. F. and Gerber, Ch., *Phys. Rev. Lett.*, 1986, **56**, 930–936.
41. Best, R. B. and Clark, J., *Chem. Commun.*, 2002, pp. 183–192.
42. Rief, M., Gautel, M., Cesterhelt, F., Fernandez, J. M. and Gaub, H. E., *Science*, 1997, **276**, 1109–1112.
43. Shao, L., Tao, N. J. and Leblanc, R. M., *Chem. Phys. Lett.*, 1997, **273**, 37–41.
44. Carrion-Vazques, M., Oberhauser, A. F., Fowler, S. B., Marszalek, P. E., Broedel, S. E., Clarke, J. and Fernandez, M., *Proc. Natl. Acad. Sci. USA*, 1999, **96**, 3694–3699.
45. Hansma, P. K. *et al.*, *Appl. Phys. Lett.*, 1994, **64**, 1738–1740.
46. Han, W., Lindsay, S. M. and Jing, T., *Appl. Phys. Lett.*, 1996, **69**, 4111–4113.
47. Kuznetsov, A. M. and Ulstrup, J., *J. Chem. Phys.*, 1991, **157**, 25–33.
48. Kuznetsov, A. M., Sommer-Larsen, P. and Ulstrup, J., *Surf. Sci.*, 1992, **275**, 52–64.
49. Snyder, S. R. and White, H. S., *J. Electroanal. Chem.*, 1995, **394**, 177–185.
50. Han, W. *et al.*, *J. Phys. Chem.*, 1997, **101**, 10719–10725.
51. Kharkats, I. Y., Kuznetsov, A. M. and Ulstrup, J., *J. Phys. Chem.*, 1995, **99**, 13545–13554.
52. Schmickler, W. and Widrig, C., *J. Electroanal. Chem.*, 1992, **336**, 213–221.
53. Friis, E. P., Kharkats, Yu. I., Kuznetsov, A. M. and Ulstrup, J., *J. Phys. Chem. A*, 1998, **102**, 7851–7859.
54. Kuznetsov, A. M. and Ulstrup, J., *J. Phys. Chem. A*, 2000, **104**, 11531–11540.
55. Tao, N. J., *Phys. Rev. Lett.*, 1996, **76**, 4066–4069.
56. Friis, E. P., Kharkats, Y. I., Kuznetsov, A. M. and Ulstrup, J., *J. Phys. Chem. A*, 1998, **102**, 7851.
57. Kuznetsov, A. M., Sommer-Larsen, P. and Ulstrup, J., *Surf. Sci.*, 1992, **275**, 52–64.
58. Zhang, J. *et al.*, *J. Phys. Chem.*, 2002, **106**, 1131.
59. *Scanning Probe Microscopy and Spectroscopy* (ed. Bonnell, D.), Wiley-VCH, 2001.
60. *Copper Proteins and Copper Enzymes* (ed. Lontie, R.), CRC Press, Boca Raton FL, 1984, p. 1.
61. Watenpaugh, K. D., Sieker, L. C. and Jensen, L. H., *J. Mol. Biol.*, 1979, **131**, 509–522.
62. Poulos, T. L., Finzel, B. C. and Howard, A. J., *Biochemistry*, 1986, **25**, 5314–5322.
63. Leggett, G. J., Davies, M. C., Jackson, D. E., Roberts, C. J, Tendler, S. J. B. and Williams, P. M., *J. Phys. Chem.*, 1993, **97**, 8852–8854.
64. Leggett, G. J., Roberts, C. J., Williams, P. M., Davies, M. C., Jackson, D. E. and Tendler, S. J. B., *Langmuir*, 1993, **9**, 2356–2362.
65. Patel, N., Davies, M. C., Hartshorne, M. R., Heaton, J., Roberts, C. J., Tendler, S. J. B. and Williams, P. M., *Langmuir*, 1997, **13**, 6485–6490.
66. Bayburt, T. H., Carlson, J. W. and Sligar, S. G., *Langmuir*, 2000, **16**, 5993–5997.
67. Nuzzo, R. G. and Allara, D. L., *J. Am. Chem. Soc.*, 1983, **105**, 4481–4483.
68. Pochapsky, T. C., Ratnaswamy, G. and Patera, A., *Biochemistry*, 1994, **33**, 6433–6441.
69. Tersoff, J. and Hamann, D. R., *Phys. Rev. B*, 1985, **31**, 805–813.
70. Pethig, R., *Dielectric and Electronic Properties of Biological Materials*, Wiley, New York, 1979.
71. Polymeropoulos, E. E., *J. Appl. Phys.*, 1987, **48**, 2404–2407.
72. Binnig, G., Rohrer, H., Gerber, C. and Weibel, E., *Physica*, 1982, **109/110B**, 2075–2077.
73. Sautet, P., *Chem. Rev.*, 1997, **97**, 1097–1116.
74. Tersoff, J. and Hamann, D. R., *Phys. Rev. Lett.*, 1983, **50**, 1998–2001.
75. Tersoff, J. and Hamann, D. R., *Phys. Rev. B*, 1985, **31**, 805–813.
76. Lang, N., *Phys. Rev. Lett.*, 1985, **55**, 230–233.
77. Lang, N., *Phys. Rev. B*, 1987, **36**, 8173–8176.
78. Lang, N., *Phys. Rev. B*, 1986, **34**, 5947–5950.
79. Lang, N., *Phys. Rev. Lett.*, 1986, **56**, 1164–1167.
80. Lang, N. D., *Solid State Phys.*, 1973, **28**, 225–299.
81. Joachim, C. and Gimzewski, J. K., *Europhys. Lett.*, 1995, **30**, 409–414.
82. Lindsay, S. M., Jing, T. W., Pan, J., Lampner, D., Vaught, A., Lewis, J. P. and Sankey, O. P., in *Nanoscale Probe of the Solid/Liquid Interface* (eds Gewirth, A. A. and Siegenthaler, H.), vol. 288, NATO ASI Series, Series E: Applied Sciences, 1995, pp. 25–43.
83. Schmickler, W. and Henderson, D., *J. Electroanal. Chem.*, 1990, **290**, 283–291.
84. Schmickler, W., *Surf. Sci.*, 1995, **335**, 416–421.
85. Vaught, A., Jing, T. W. and Lindsay, S. M., *Chem. Phys. Lett.*, 1995, **236**, 306–310.
86. Morgan, H. and Pethig, R. J., *J. Chem. Soc. Faraday Trans.*, 1986, **82**, 143–146.
87. Parker, M., Davies, M. C. and Tendler, S. J. B., *J. Vac. Sci. Technol. B*, 1996, **14**, 1432–1436.
88. Onuchic, J. N. and Beratan, D. N., *J. Chem. Phys.*, 1990, **92**, 722–733.
89. Gruschus, J. M. and Kuki, A., *J. Phys. Chem.*, 1993, **97**, 5581–5593.
90. Lindsay, S. M., Sankey, O. F., Li, Y., Herbst, C. and Rupprecht, A., *J. Phys. Chem.*, 1990, **94**, 4655–4660.
91. Sieker, L. C., Stenkamp, R. E. and LeGall, J., *Methods Enzymol.*, 1994, **243**, 203–223.
92. Claypool, C. L., Faglioni, F., Goddard, W. A., Gray, H. B., Lewis, N. S. and Marcus, R. A., *J. Phys. Chem. B*, 1997, **101**, 5978–5995.
93. Cyr, D. M., Venkataraman, B., Flynn, G. W., Black, A. and Whitesides, G. M., *J. Phys. Chem.*, 1996, **100**, 13747–13759.

ACKNOWLEDGEMENTS. I thank Professors H. A. O. Hill, G. W. Canters, J. Meyer and L. L. Wong, and Drs P. Kyritsis, K. K. Lo and W. Xie for helpful discussions, providing the proteins and laboratory facilities. Financial support from a Felix fellowship is gratefully acknowledged.

Received 19 December 2002; revised accepted 11 February 2003